Evapotranspiration deficit controls net primary production and growth of silver fir: implications for Circum-Mediterranean forests under forecasted warmer and drier conditions

Vicente-Serrano, S.M.[1,*], Camarero, J.J.[1], Zabalza, J.[1], Sangüesa-Barreda, G [1], López-Moreno, J.I. [1] and Tague, C.L.[2]

[1]Instituto Pirenaico de Ecología, Consejo Superior de Investigaciones Científicas, IPE-CSIC. Avda Montañana 1005. Zaragoza 50059, Spain.

[2]University of California, 2400 Bren Hall, Santa Barbara 93106-5131, USA.

*corresponding author, Sergio M. Vicente-Serrano, Tel: +34 976369393 (ext. 880053), e-mail: svicen@ipe.csic.es

Abstract

Warming-induced drought stress has been hypothesized as a major driver of forest net primary production (NPP) reduction, but we lack reliable field data to assess if higher temperatures lead to forest NPP reduction, particularly in humid sites and at basin to landscape spatial scales. The use of a landscape approach would allow considering the feedbacks operating between climate, topography, soil vegetation and water resources. Here we follow that approach by simulating NPP using the Regional Hydro-Ecologic Simulation System (RHESSys) model and by comparing the results with radial growth data (tree-ring widths and intrinsic water-use efficiency −iWUE). We evaluate the relationships between climate, growth, NPP, atmospheric CO_2 concentrations (c_a) and iWUE in xeric and mesic silver fir forests subjected to contrasting water balances. The growth data successfully validated the 11-month NPP cumulated until spring. The main negative climatic driver of growth and NPP was the summer evapotranspiration deficit, which shows a negative association with tree-ring width indices. Sensitivity analyses indicate that rising c_a do not compensate the severe NPP reduction associated to warmer and drier conditions. The positive effect of rising c_a on NPP is mediated by climatic site conditions being detected only in mesic sites, whereas the negative effects of drought on NPP override any c_a-related enhancement of NPP in xeric sites. Future warmer and drier conditions causing a higher evaporative demand by the atmosphere could lead to a NPP decline in temperate conifer forests subjected to episodic droughts.

Key words: climate warming, tree-ring, *Abies alba*, Regional Hydro-Ecological Simulation System (RHESSys), Pyrenees, drought stress, silver fir.

Introduction

Water deficit is likely to increase if climate warms and both drying and warming trends could lead to a reduction in net primary production (NPP) and growth of forests (Allen et al., 2010; Carnicer et al., 2011). Some studies already suggest that warming-related aridification trends are causing NPP reductions in forests subjected to contrasting water balances including semiarid (Breshears et al., 2005; Adams et al., 2009; Williams et al., 2013), boreal (Peng et al., 2011), temperate (van Mantgem and Stephenson, 2007) or tropical biomes (Phillips et al., 2010). However, there are still many research gaps on the roles played by rising temperatures and increased evapotranspiration levels on NPP and growth of forests under current and future climatic conditions.

Comparing NPP and growth responses to observed and forecasted climate and emission scenarios in sites with different water balances could aid to determine if temperature or precipitation are the major drivers of NPP and growth. Rising atmospheric CO_2 concentrations (c_a) may also affect NPP and growth by improving the intrinsic water-use efficiency (iWUE, i.e. ratio of net assimilation to stomatal conductance), but improved iWUE has not translated into enhanced growth neither in xeric nor in mesic sites (Peñuelas et al. 2011, Lévesque et al. 2014). So, the question remains open about which climatic factors and c_a levels would mainly drive NPP and growth.

The synergistic effects of warmer and drier conditions could also lead to reduction in NPP and growth across multiple spatial scales. Furthermore, a reduction in growth and NPP could lead to defoliation with cascading effects on hydrological processes at the basin and landscape levels (run-off, groundwater recharge, streamflow, etc.) (Guardiola-Claramonte et al. 2011, Anderegg et al., 2013). These complex feedbacks call for an integrated evaluation of landscape-level forest responses to climate warming including drought and related hydro-ecological processes. These assessments

should consider nonlinear NPP and growth responses to future warmer and drier climatic conditions (Lloyd et al. 2013), including novel climatic or emission scenarios or unprecedented events (e.g., severe droughts).

In the Mediterranean Basin and also in Spain there is an increase in the frequency and severity of droughts (Hoerling et al., 2012). For instance, during the last 50 years there has been a persistent decrease of surface relative humidity of the growing season in mainland Spain associated with a marked warming trend, which caused increased atmospheric evaporative demand (Vicente-Serrano et al., 2014). Projections indicate an even higher warming trend and a decrease in precipitation across the Western Mediterranean Basin (Giorgi and Lionello, 2008).

Recent climate variability have caused widespread drought-linked reductions in NPP and growth of Circum-Mediterranean forests both in dry (Sarris et al., 2007; Vicente-Serrano et al., 2010a; Barbeta et al., 2013) and mesic sites (Jump et al., 2006; Linares and Camarero, 2012a, 2012b). In Iberian pine forests warming-induced drought stress particularly affected growth and survival of those species with higher xylem vulnerability to cavitation (Sánchez-Salguero et al., 2012) or those populations living in the driest sites (Martínez-Vilalta and Piñol 2002, Martínez-Vilalta et al., 2008). However, other authors have noted either a remarkable capacity of tree populations from drought-prone areas to adapt to water shortage by changing growth dynamics and water use (Alla and Camarero, 2012; Granda et al. 2014) or a high sensitivity to dry periods in humid sites (Büntgen et al., 2013).

Such apparently contradictory findings can be resolved by upscaling physiological models of photosynthetic activity, growth or NPP (e.g., Sabaté et al., 2002) to a basin level thus integrating the complex interactions between climate, c_a, forests and soil hydrological processes (Tague and Band, 2004; Tague et al. 2009a and

b). In this sense, hydro-ecological models considering tree processes as constrained by climate and water availability allow simulating forest responses (NPP, growth, carbon and water use) to observed and projected warming at basin to landscape scales (Morales et al., 2005; Medlyn et al. 2011). Here, we use a hydro-ecological model to understand the causes of the observed and simulated NPP and growth year-to-year variability of silver-fir (*Abies alba*) at a landscape level in the Spanish Pyrenees. Hydro-ecological simulations are validated using radial-growth data obtained in a dendrochronological network. Silver-fir growth decline in that area has been observed since the 1980s in the most xeric sites, being attributed to drought stress (Camarero et al., 2002; Linares and Camarero, 2012a). Different scenarios of emission of greenhouse gases (IPCC, 2007) indicate that forecasted regional warming may vary between +2.8ºC and +4ºC in the Pyrenees (López-Moreno et al., 2008). Further, warmer conditions and a reduction in soil water resources (López-Moreno et al., 2009, 2011) are expected to intensify in late summer, when silver-fir is particularly sensitive to dry conditions (Camarero et al., 2011; Pasho et al., 2011).

Material and methods

Study area

The study area is the upper Aragón river Basin located in the Central Spanish Pyrenees, where it occupies 1432 km^2 and has a mean elevation of 1170 m a.s.l. (Fig. 1). In that area there is a marked precipitation gradient as elevation increases northwards where more humid and cool conditions prevail (mean total precipitation of 1600-2000 mm; see Supporting Information, Fig. S1). Less wet and warmer (more xeric) sites are located at lower elevation southwards (total precipitation of 750-900 mm) (Fig. 1). The wet seasons are spring and fall while summer is the driest season (Cuadrat et al. 2007). The

mean annual temperature at 1100 m of elevation is 8º C while the 0º C-isotherm (above which snow persists) is located at 1600 m from November up to April.

Mountain forests of the study area located between 900 and 2000 m are dominated by conifer species (*Pinus sylvestris* L., *Pinus uncinata* Ram.) whose abundance changes along climatically-related altitudinal levels. Silver fir (*Abies alba* Mill.) is one of the tree species reaching larger biomass and height (up to 40 m) in this area, where it reaches its southwestern distribution limit, and it is dominant in northern and northwestern humid slopes with deep soils formed on marls, limestones or glacial deposits (Camarero et al., 2011). Silver fir appears forming pure forests and also mixed stands with Scots pine and beech (*Fagus sylvatica* L.). Pyrenean silver-fir forests were moderately exploited for timber extraction until the 1950s (Cabrera, 2001).

Datasets used as inputs of the model

To model growth and NPP in each forest, we used homogenised climatic series of daily data (mean maximum and minimum temperatures, total precipitation) for the period 1979-2006 (Vicente-Serrano et al., 2010b; El Kenawy et al., 2011). These data were obtained from stations located near each study site (see Supporting Information, Fig. S2). The observed monthly atmospheric CO_2 levels (c_a) were also included in the model. They were obtained from the Mauna Loa (Hawaii, USA) station (http://cdiac.ornl.gov/ftp/trends/co2/maunaloa.co2) and interpolated daily. We used several geographical sources of information. First, we used a digital elevation model (25-m resolution, Environment Department, Aragón Regional Government) to describe the topographical features of the study area. Second, forest and land-cover types were obtained from the Spanish National Forest Map and the Third National Forest Inventory (period 1996-2006) (Supporting Information, Fig. S2). Third, soil classes were taken

144 from the European Soil Database (available at http://eusoils.jrc.ec.europa.eu/; Wösten et
145 al. 1999; Jones et al. 2004, Panagos et al. 2012). Finally, daily streamflow data were
146 obtained from a gage station located at the end of the Yesa reservoir (see Fig. 1).
147
148 *The RHESSys hydro-ecological model*
149 We used the Regional Hydro-Ecological Simulation System version 5.14.5 (hereafter
150 RHESSys, see http://fiesta.bren.ucsb.edu/~rhessys) to model NPP in the study forests
151 (Tague and Band 2004). We assume that radial growth and stem wood production,
152 which is a major carbon sink of the biosphere, would be reliable surrogates of NPP as
153 has been observed at large spatial scales (Malmström et al. 1997). RHESSys is a hydro-
154 ecological model designed to capture the bidirectional fluxes (feedbacks) of
155 hydrological and ecological (carbon and water use by vegetation) processes and their
156 spatial patterns within basins (Tague and Band, 2004). In mountains, topography drives
157 hydrological processes and vegetation dynamics through indirect effects on energy
158 drivers (radiation, temperature), and moisture redistribution and storage (soil moisture)
159 that influence carbon cycling and water use.
160 RHESSys allows analyzing the hydro-ecological interactions at several spatial
161 scales from a hillslope to whole basins (Band et al. 1993). The model computes
162 different hydrological, climatic and vegetation processes at related patch scales and
163 allows upscaling them to the landscape. RHESSys couples an ecosystem carbon cycling
164 model with a spatially distributed hydrology model. Details of the model are provided
165 by Tague and Band (2004) and more recent refinements of energy, moisture and carbon
166 cycling model are described on RHESSys website. A brief overview is given here.
167 Forest energy processing in RHESSys accounts for sunlit/shaded partitioning and both
168 overstory and understory radiation absorption. Photosythesis is based on the Farquhar

169 equation (Farquhar and Von Caemmerer, 1982) and stomatal conductance estimates
170 include regulation by vapor pressure deficit, rooting zone soil moisture, air temperature
171 and other environmental controls. The reference evapotranspiration is estimated by
172 using the FAO-56 Penman-Monteith equation (Allen et al., 1998), based on minimum
173 temperature and daily temperature data used to estimate vapor pressure deficit and solar
174 radiation, respectively. Wind speed is set as constant and equal to 2 m s^{-1}. Estimates of
175 NPP are allocated to growth of different plant components including leaves, stems and
176 roots following the approach of Dickinson et al. (1998). Vertical hydrologic processes
177 include estimates of canopy, litter and soil evaporation and transpiration. Soil
178 infiltration and drainage through rooting zone and unsaturated and saturated stores are
179 influenced by soil parameters that are typically calibrated as described in more detail
180 below. Lateral moisture redistribution is based on topography and local soil properties.
181 Climate drivers in RHESSYs are spatially interpolated based on the Mountain Climate
182 Simulator (MTN-CLIM), specifically designed to deal with microclimatic conditions in
183 topographically complex areas (Running et al., 1987). The RHESSys model has been
184 previously used to simulate NPP in different vegetation types including mountain
185 grasslands (Mitchell et al., 2005), and high-elevation ecosystems (Christensen et al.,
186 2008). Applications of the model to forests can be found in other studies (Grant et al.,
187 2013; Tague and Peng, 2013). Of particular relevance to this study is a recent
188 application of RHESSYs in the American Southwest where model estimates were
189 shown to accurately represent spatial patterns of both productivity and drought related
190 mortality along an elevational gradient. (Tague et al. 2013).
191 Soil parameters in RHESSys typically require calibration since soil and geologic
192 inputs do not account for complex controls on drainage rates such as hillslope scale
193 preferential flow path distributions. Calibration adjusts parameters controlling the

194 storage and drainage rates of water flow through the soil, namely the saturated hydraulic
195 conductivity at the surface (*K*) and its decay with depth (*m*). Parameters were adjusted
196 by using a Monte-Carlo procedure based on 1600 simulations run for the period 1996-
197 2006. We selected those parameters that produced monthly streamflow estimates that
198 gave a value of higher than 0.7 for the Nash-Sutcliffe (NSE) model efficiency
199 coefficient (Nash and Sutcliffe, 1970) when compared with observed monthly
200 streamflow. To assess the calibration quality we also used other performance statistics
201 recommended by Moriasi *et al*. (2007), such as the Pearson correlation coefficient
202 calculated between observed and simulated data (*r*), the percent bias (PBIAS) and the
203 ratio of the root mean square error to the standard deviation of measured data (RSR).
204 PBIAS higher than -15% and RSR values lower than 0.07 indicate an adequate
205 calibration of the model (Singh et al., 2004).
206
207 *Growth and water-use efficiency data*
208 To validate and compare observed and simulated growth data we obtained annual radial
209 growth data from a previously established dendrochronological network. Stem wood
210 production and radial growth are regarded as good proxies of changes in forest NPP
211 (Zweifel et al. 2010). We used data from eight silver-fir forests located across wide
212 altitudinal and climatic gradients covering the study area and including forests with
213 different defoliation and mortality levels (Fig. 1). To describe recent vigour levels of the
214 study sites stand die-off levels (percent crown defoliation, living or dead status) were
215 estimated in the field by sampling 15 dominant trees per stand (trees were randomly
216 selected across a 500-m long and 20-m wide transect) during 1999-2001 and 2013 to
217 differentiate declining (sites with more than 25% trees with crown defoliation >50%;
218 e.g., sites PE and LO) and non-declining (e.g. sites SO and SO) stands. The percentage

of crown defoliation was visually estimated using a semi-quantitative scale (see further details on tree sampling in Camarero *et al*. (2011). We obtained site chronologies of standardized and detrended tree-ring width indices based on the average of 15 trees sampled in each study site (period 1982-2000), and the average of all 8 measurement sites was calculated to obtain a regional chronology.

We also estimated a mean regional iWUE series for the period 1982-2000 by averaging two series developed for two forests subjected to xeric (site JP) or mesic (site SO) conditions (see Fig. 1). The annual iWUE was estimated by calculating the carbon isotopic discrimination of wood cellulose obtained from annually-resolved tree rings (see more details on sampling and analyses in Linares and Camarero 2012b).

Statistical analyses

To evaluate the quality of monthly NPP estimates from RHESSys (obtained by summing daily NPP values) accumulated for different time scales (1 up to 24 months), we compared them with annual growth data using the Pearson correlation coefficient. This was done for local and mean regional NPP and growth series. We computed correlations between tree ring growth estimates and different estimates of accumulated NPP for different accumulation periods in the year associated with the corresponding tree ring measurement. We note that this approach helps to reduce uncertainty due to complex within seasonal patterns of allocation of NPP to specific plant component including stem wood that are poorly understood. Then, we quantified the relationships between climate and growth or NPP. We used the following monthly climatic variables: total precipitation (P), mean air temperature (T), reference (ETo) and actual (ET) evapotranspiration. We also calculated the climatic water balance (difference between P and ETo) since it is a widely used measure of climatic aridity and drought (Vicente-

Serrano et al., 2010c; 2012a). Lastly, we obtained the evapotranspiration deficit (difference between ETo and ET) because it has a high explicative power of vegetation distribution at global scale (Stephenson, 1990). Furthermore, this last measure has been shown to affect radial growth of conifer species in central Europe (Lévesque et al., 2013).

Sensitivity analyses under climate change scenarios

We performed sensitivity analyses of the RHESSys outputs after validating the NPP series as reliable proxies of the spatiotemporal variability in growth of the studied Pyrenean forests. Several plausible climatic scenarios for the study area were used as model forcing (López-Moreno et al., 2008). We used twelve regional climate models obtained from the ENSEMBLES project for the A1B IPCC emission scenario (Hewitt and Griggs, 2007). These models included wide ranges of forecasted temperature increase (from +1.0º up to +3.1º C for the year 2050) and precipitation change (from +0.5% up to –28.3% for the year 2050) for the study area. The model RHESSys was forced by considering a linear increase of temperature (from 0º to +3º C) and a wider range of precipitation change (from –20% to +20%) to take into account the uncertainty of climatic projections. We also used the average multi-model projections for the evolution of the estimated c_a considering the A1B emission scenarios for the year 2050, namely an increase of +30% of c_a (Solomon et al., 2007). We obtained twelve NPP simulations for each forest as a result of combining different temperature and precipitation changes.

Results

Model calibration and NPP-growth association

The model RHESSys successfully predicted monthly streamflow data according to the calibration and verification statistics calculated for two different time periods (Table 1, Supporting Information, Fig. S3). This was confirmed by the tight positive association (r = 0.81, P < 0.01) found between the regional silver-fir growth series and the simulated NPP accumulated during 19 months before April of the year of tree-ring formation (Fig. 2). The highest correlations between observed growth and cumulative NPP estimates were observed by using accumulation for 10-18 months prior to March to June of the year associated with the tree-ring based growth estimate (Supporting Information, Fig. S4). The simulated NPP captures the severe silver-fir growth decline observed in 1986 quite well. This drought event is related to the beginning of die-off in the area during the mid 1980s (see Camarero et al., 2011). Particularly large growth increases such as those observed in 1993 are also reasonably represented by the NPP series simulated by RHESSys. The positive association between radial growth and NPP was also observed at the site scale, being particularly strong in sites showing die-off and subjected to moderate water deficit (e.g., sites PE, LO) (Fig. 3).

Climate impacts on NPP, growth and iWUE

Regional scale evapotranspiration deficit (ETo-ET) was negatively related to the regional tree-ring width (r = -0.79, P<0.01) and NPP series (r = -0.83, P<0.01) but positively (despite weakly, r = 0.46, P<0.05) associated to iWUE, i.e. drier conditions induced lower radial growth and higher iWUE in silver-fir forests (Fig. 4). Consequently, growth and iWUE were negatively associated (r = -0.59, P < 0.05) as NPP and iWUE were (r = -0.72, P < 0.01).

The strongest correlation, in absolute terms, between regional NPP and regional climatic variables was found for summer actual evapotranspiration (ET) and the

evapotranspiration deficit which presented negative associations for summer months and at 1-10 month long scales (Fig. 5a). Simulated NPP was positively (negatively) related to spring (summer) ETo, particularly at 1-6 months long scales (Fig. 5a). Summer precipitation was also positively associated to NPP at similar temporal scales, whereas temperature affects NPP at shorter scales with different signs depending on the season (positive in winter, negative in summer). Regarding growth, again the actual and reference evapotranspirations and the evapotranspiration deficit were negatively related to stemwood production at similar months and scales as the NPP was (Fig. 5b). The correlations between climatic variables and NPP accumulated until June were similar to those found for growth (*results not presented*). These results indicate that water deficit, summarized by the difference between the actual and the reference evapotranspiration, mainly controls NPP and growth.

The results observed at the regional scale concurred with those observed at the local scale in two sites characterized by different water balances and recent die-off intensity (JP *vs*. SO sites). Specifically we compared the xeric site JP (annual water balance, i.e. P-ETo, of 39 mm) which shows die-off and the mesic site SO (annual water balance of 950 mm) which does not present die-off (see Supporting Information, Fig. S1). In the xeric site JP the positive correlations between summer precipitation and NPP or radial growth were higher than in the mesic site SO (Supporting Information, Fig. S5). High late-winter and spring temperatures were positively related to enhanced NPP and growth during a longer period in the xeric than in the mesic site. Contrastingly, the actual evapotranspiration (ET) was more strongly related to NPP in the mesic than in the xeric site. Summer temperatures were more tightly related to growth in the xeric than in the mesic site, particularly during long time scales (8-10 months). Overall, the evapotranspiration deficit (ETo-ET) was the most important driver of NPP and growth

in these two compared sites, since increased deficit lead to decreased NPP and growth. In this case the strongest associations between the evapotranspiration deficit and NPP or growth were detected at shorter temporal scales in the xeric than in the mesic site.

NPP responses to forecasted climatic scenarios

The three assessed climatic scenarios (warming, precipitation decline, warming and precipitation decline) show different effects on simulated NPP (Fig. 6). There is also some influence of rising c_a on NPP since the combined control climate and higher c_a scenario (C+CO_2 scenario in Fig. 6) increases NPP by 5.7% in comparison to control climate (C). Nevertheless, there is not a clear pattern in the NPP responses to forecasted climatic and CO_2 conditions considering either the most climatically favourable or unfavourable years. For instance, the C+CO_2 scenario shows more NPP in some favourable years (e.g., 1987) but not in others (e.g., 1997 and 2003). Considering climatically unfavourable years the difference between scenarios is not important (e.g., 1986).

Focusing on the climate change scenarios, a warmer climatic scenario (TC) would enhance NPP by +3.2%, whereas a climatic scenario characterized by drier conditions (PC) would decrease NPP by −4.1%. A warmer and drier scenario (AC) would increase NPP by +1.1% in relation to the control period. All these climatic change scenarios consider the 2050s projected atmospheric CO_2 concentrations. This means that in average the CO_2 increase could compensate the increase in evaporation if precipitation maintains the levels for the control scenario (C), but this compensation is not observed for an scenario with a 20% of precipitation reduction. All three climatic scenarios would lead to more severe NPP reductions than the C+CO_2 scenarios during the years recording unfavourable climate conditions like in 1984, 1994, 1995, 1996,

1998 and 2001. The exception is 1986, in which the C+CO_2 scenario provides similar NPP decrease than the three climate scenarios. Probably the very dry 1986 conditions were so limiting for NPP and growth that the role of rising c_a on NPP could be considered negligible. In the case of favourable years, the influence of rising c_a on NPP is complex since although in some years the projected NPP values under elevated c_a are higher than those projected under different climate forcing scenarios (e.g., 1987, 1990), during other favourable years (e.g., 1997) the pattern is the opposite. In any case, the general pattern observed is that warmer and drier conditions would lead to NPP reduction during unfavourable climate years, thus overriding any expected NPP compensation due to rising c_a during those years.

Nevertheless, in average and regionally rising c_a shows increased NPP that seems to compensate the effects of projected climate changes on NPP. Stable temperatures and a +20% increase in precipitation led to a noticeable NPP enhancement (+6%). Considering +1 and +3 ºC warmer scenarios as compared with the period of control, the simulated NPP shows a positive response to warming but negative for drying trends (Supporting Information, Fig. S6). Nevertheless, the impact of the temperature rise on NPP does not seem to be linear and it depends on water availability. For example, NPP increases (+6% regarding control) with higher precipitation levels (+20%) and warmer conditions (+1ºC) are lower than those predicted (+4%) for the same precipitation levels but under much warmer conditions (+3ºC). Under a strong reduction of precipitation (-20%), NPP changes are also expected to be positive given rising c_a, but higher temperature scenarios (+3ºC) would compensate rising c_a, and lead to NPP values similar to those predicted for control scenarios.

Comparing results for the two forests with contrasting climatic conditions and die-off intensity (JP, more xeric site showing die-off; SO, mesic site without die-off),

there are strong differences in the estimated NPP response to the increase in c_a for the different climate scenarios (Supporting Information, Fig. S7). The mesic site SO shows strong NPP enhancement (+36%) as a response to increased c_a and control climate conditions. The different climate scenarios show NPP reductions in comparison to the C+CO_2 scenarios but they show strong NPP increases in comparison to control climate conditions (see scenarios in Fig. 6): +21.6% in a warmer scenario (TC); +28.7% in a drier scenario (PC); and +12.3% in response to combined warmer and drier conditions. Thus, the increase in c_a could compensate the negative effects of warmer and drier conditions (AC) on NPP even during the most stressful years (e.g., severe drought years).

In contrast, in the xeric site (JP), the positive effect of rising c_a on NPP under control climate conditions is very low (+0.6%) and does not compensate the NPP reduction associated to warmer (TC, NPP reduced by −0.5%) and warmer and drier (AC, NPP reduced by −0.8%) forecasts, with the exception of the drier (PC) scenarios, which shows +0.6% NPP higher than the control climate. In the xeric site the NPP reductions correspond with years characterized by warm and dry conditions such as those observed in 1986 and during later droughts (1995-1996). Those conditions caused intense growth and NPP declines, widespread defoliation and mortality, thus triggering die-off episodes (see details in Linares and Camarero, 2012a). Our findings indicate that those defoliation and die-off episodes would be more frequent under warmer and drier climatic scenarios. Note also that in the xeric site NPP values were always lower than in the mesic site, confirming that growth and NPP are closer to the climatic threshold of defoliation and die-off (negative NPP) in the xeric site.

Discussion and conclusions

We analyzed the impacts of different climatic scenarios and increasion c_a on NPP of Pyrenean silver-fir forests to infer how the forecasted future warmer and drier conditions would impact the growth, productivity and persistence of these rear-edge forests. This simulation approach was based in a hydro-ecological model (RHESSys) that accounts for climate-soil-vegetation feedbacks at a landscape level. The model was further validated with field data of radial growth obtained from forests growing under contrasting climatic conditions and showing different levels of die-off symptoms (defoliation, growth loss and mortality). The validation was successful at the regional (basin) and local (site) levels since the NPP accumulated until April-May and tree-ring width were highly correlated. Recent studies have also pointed out that these models are valuable tools to predict NPP and growth of forests and indicate that annual ring widths are good predictors of changes in NPP (Kong et al., 2012; Peng et al., 2012; Poulter et al., 2013). Such connection between NPP and radial growth has also been observed at continental scales in Europe (Babst et al., 2013).

Growth and NPP are tightly coupled at annual scales but this association disappears at monthly or daily scales (Zweifel et al., 2010). This is in agreement with the fact that wood production is the result of accumulating the surplus of synthesized carbohydrates, and therefore secondary growth and carbon storage reflect cumulative NPP (Gough et al., 2008). Growth and NPP may not be coupled at short temporal scales, since wood formation is just one aspect of tree growth and carbon must first be used for primary growth to form shoots, buds, leaves and roots (Stoy et al., 2009). In dendrochronology, it is also well established that the climatic conditions of the previous year greatly determine, probably through the synthesis and storage of carbohydrates, the tree-ring width of the following growing season (Fritts, 2001). Thus our finding that radial growth was highly correlated with estimated NPP accumulated during the 11

months before June, is consistent with dendrochronological findings and this mechanistic explanation. We found that correlations between model estimates of NPP and stem growth are better for less productive sites. This is in agreement with the results by Tague et al. (2013), which suggest that in more productive years, plant allocation strategies vary in ways that may not be accurately represented in the model. In the Pyrenees the highest radial-growth rates of silver fir typically occur in May and June (Camarero et al., 2011).

Our empirical analysis of the climate drivers and growth suggest that water deficit, and particularly the difference between the evaporative demand by the atmosphere and the available water to evaporate, determine growth and NPP in the study sites. These climatic parameters were also proposed by Lévesque *et al*. (2013) to explain the inter-annual variability of growth and the vulnerability to drought of conifers inhabiting central-European forests. We note however correlations between RHESSys model estimates and growth were higher than correlations associated with climate-based metrics. This is expected given that the model accounts for both within season temporal patterns of climate drivers and includes a semi-mechanistic representation of plant physiological responses to climate deficits and vegetation conditions.

Both RHESSys estimates and empirical climate metrics suggest a high sensitivity of forests in this region to drought, at the regional scale and for both mesic and xeric sites. The described sensitivity to drought is remarkable given that we included forests located in relatively humid study sites that always showed positive water balances. We note however that plant communities dominating wet sites are also vulnerable to water deficit, in terms of xylem cavitation, because they seem not to be adapted to severe water shortage (Maherali et al., 2004). Furthermore, other studies

444 based on tree-ring data and remote sensing have shown that NPP and growth responses
445 to drought also occur in these humid sites (Pasho et al., 2011; Vicente-Serrano et al.,
446 2012b).

447 The declines in NPP and growth shown here suggest that a warming-related
448 higher evaporative demand and lower available soil moisture could cause growth
449 decline during the most climatically unfavourable years. In fact, the associations
450 observed between growth and the evapotranspiration deficit (ETo-ET) were higher than
451 those observed with other climatic variables such as mean temperature or total
452 precipitation (Camarero et al., 2011; Linares and Camarero, 2012a). Evapotranspiration
453 deficit not only caused growth and NPP declines but also increased water-use
454 efficiency. However, growth and NPP were more related to the atmospheric demand
455 than water-use efficiency. Our findings agree with previous reconstructions of growth
456 and water-use efficiency showing that they are neither related in silver fir (Linares and
457 Camarero 2012b) nor in other conifer species (Lévesque et al. 2014). If rising c_a leads to
458 increased water-use efficiency through a reduction in stomatal conductance this does
459 not imply an enhancement in tree growth, even in the case of xeric sites where a higher
460 improvement in water-use efficiency would be expected (Peñuelas et al. 2011). Our
461 findings suggest that the negative effects of increasing evapotranspiration deficit on
462 NPP in a warmer and drier scenario will override any positive effect of rising c_a on NPP
463 in xeric sites where ongoing die-off episodes are already being observed (Camarero et
464 al. 2011).

465 Most die-off episodes of Pyrenean silver-fir forests have been detected in
466 marginal dry areas, usually constituting one of the southernmost distribution limits (rear
467 edge) of the species in Europe (Camarero et al. 2011). Our model estimates similarly
468 show lower NPP, and in some cases negative NPP values in the xeric study. Although

469 increasing atmospheric CO_2 levels coincide with enhanced tree growth and NPP as our
470 model shows, our results also indicate that strong NPP reductions corresponding to
471 climatically unfavorable years would become common in humid areas if current
472 warming trends continue, despite an increase in c_a and possibly improved water-use
473 efficiency. Moreover, in xeric sites the strong NPP reductions are predicted to be more
474 severe and frequent as a response to warmer and drier conditions, even if c_a rises.

475 In the long term this study predicts a general increase of NPP in silver-fir forests
476 as a response to rising c_a. Nevertheless, warmer climatic scenarios enhancing
477 atmospheric evaporative demand would limit NPP more strongly than drier ones. Thus,
478 warmer conditions may cause growth decline and trigger die-off of xeric Pyrenean
479 silver-fir forests despite improved water-use efficiency (Linares and Camarero, 2012b).
480 Ecophysiological models predict a general decrease of NPP in Circum-Mediterranean
481 forests if warming and drying trends are maintained (Anav and Mariotti 2011). Hydro-
482 ecological models represent valuable tools to predict the forest dynamics at basin and
483 landscape scales considering several forest parameters (growth, NPP and leaf area) but
484 also accounting for interactions among different climatic drivers both within and
485 between growing seasons. Further, combining simulated NPP and reconstructed growth
486 data would allow quantifying long-term trends in carbon uptake (e.g., stemwood
487 production) and water use (e.g., streamflow) and to forecast their trends under future
488 climate and biogeochemical scenarios. The latter aim is a high priority in drought-prone
489 areas such as Mediterranean forests.

490

491 **Acknowledgements**

492 We would like to thank the Spanish Meteorological State Agency (AEMET) and the
493 Confederación Hidrográfica del Ebro for providing the climatic and streamflow

494 databases used in this study. This work has been supported by research projects
495 CGL2011-27574-CO2-02, CGL2011-27536 financed by the Spanish Commission of
496 Science and Technology and FEDER, "LIFE12 ENV/ES/000536-Demonstration and
497 validation of innovative methodology for regional climate change adaptation in the
498 Mediterranean area (LIFE MEDACC)" financed by the LIFE programme of the
499 European Commission and CTTP1/12 financed by the Comunidad de Trabajo de los
500 Pirineos. JJC also acknowledges the support of ARAID and projects 012/2008,
501 387/2011 and 1012S (Organismo Autónomo Parques Nacionales, Spain).
502

503 **References**

504 Adams HD, et al. 2009. Temperature sensitivity of drought-induced tree mortality
505 portends increased regional die-off under global-change-type drought. *Proceedings*
506 *of the National Academy of Sciences USA* 106: 7063–7066.

507 Alla, A.Q. and Camarero, J.J. 2012. Contrasting responses of radial growth and wood
508 anatomy to climate in a Mediterranean ring-porous oak: implications for its future
509 persistence or why the variance matters more than the mean. *European Journal of*
510 *Forest Research* 131: 1537–1550.

511 Allen, R.G., L.S.Pereira, D. Raes, and M. Smith. 1998. Crop Evapotranspiration:
512 Guidelines for Computing Crop Water Requirements Food and Agriculture
513 Organization of the United Nations, Rome.

514 Allen CD, et al. 2010. A global overview of drought and heat-induced tree mortality
515 reveals emerging climate change risks for forests. *Forest Ecology and Management*
516 259: 660–684.

517 Anav, A. and Mariotti, A. 2011. Sensitivity of natural vegetation to climate change in
518 the Euro-Mediterranean area. *Climate Research* 46: 277–292.

519 Anderegg, W. R. L., J. Kane, and L.D.L. Anderegg. 2013. Consequences of widespread
520 tree mortality triggered by drought and temperature stress. Nature Climate Change
521 3: 30–36

522 Babst, F., Poulter, B., Trouet, V., Tan, K. et al. 2013. Site- and species-specific
523 responses of forest growth to climate across the European continent. *Global Ecology*
524 *and Biogeography* 22: 706–717.

525 Band, L.E., Patterson, P., Nemani, R. and Running, S.W. 1993. Forest ecosystem
526 processes at the watershed scale: incorporating hillslope hydrology. *Agricultural and*
527 *Forest Meteorology* 63: 93–126.

528 Barbeta, A., Ogaya, R. and Peñuelas, J. 2013. Dampening effects of long-term
529 experimental drought on growth and mortality rates of a Holm oak forest. *Global*
530 *Change Niology*, doi: 10.1111/gcb.12269.
531 Breshears, D.D., N.S. Cobb, P.M. Rich, K.P. Price, C.D. et al. 2005. Regional
532 vegetation die-off in response to global-change type drought. *Proceedings of the*
533 *National Academy of Sciences of the United States of America*. 102: 15144–15148.
534 Büntgen, U., Martínez-Peña, F., Aldea, J., Rigling, A., Fischer, E.M., Camarero, J.J.,
535 Hayes, M.J., Fatton, V. and Egli, S. 2013. Declining pine growth in Central Spain
536 coincides with increasing diurnal temperature range since the 1970s. *Global and*
537 *Planetary Change* 107: 177–185.
538 Cabrera, M. 2001. Evolución de abetares del Pirineo aragonés. *Cuadernos de la*
539 *Sociedad Española de Ciencias Forestales* 11: 43–52.
540 Camarero, J.J., Padró, A., Martín-Bernal, E. and Gil-Pelegrín, E. 2002. Aproximación
541 dendroecológica al decaimiento del abeto (*Abies alba* Mill.) en el Pirineo aragonés.
542 *Montes* 70: 26–33.
543 Camarero, J.J., Bigler, C., Linares, J.C. and Gil-Pelegrin, E. 2011. Synergistic effects of
544 past historical logging and drought on the decline of Pyrenean silver fir forests.
545 *Forest Ecology and Management* 262: 759–769.
546 Carnicer J, Coll M, Ninyerola M, et al. 2011. Widespread crown condition decline, food
547 web disruption, and amplified tree mortality with increased climate change-type
548 drought. *Proceedings of the National Academy of Sciences* 108: 1474–1478.
549 Christensen, L, Tague, C and Baron, J. 2008. Spatial patterns of simulated transpiration
550 response to climate variability in a snow dominated mountain ecosystems.
551 *Hydrological Processes* 22: 3576–3588.

552 Cuadrat, J.M., Saz, M.A. and Vicente-Serrano, S.M. 2007. *Atlas Climático de Aragón*.
553 Gobierno de Aragón, Zaragoza, Spain. 229 pp.
554 Dickinson RE, Shaikh M, Bryant R, Graumlich L (1998) Interactive canopies for a
555 climate model. Journal of Climate 11: 2823–2836.
556 El Kenawy, A., López-Moreno, J.I. and Vicente-Serrano, S.M. 2011. Recent changes in
557 daily temperature extremes in Northeastern Spain (1960-2006). *Natural Hazards*
558 *and Earth System Science*. 11: 2583–2603.
559 Farquhar GD, Von Caemmerer S (1982) Modeling of photosynthetic response to
560 environmental conditions. Encyclopedia of plant physiology 12: 549–587.
561 Fritts, H.C. 2001. *Tree Rings and Climate*. Academic Press, London.
562 Giorgi, F. and Lionello, P. 2008. Climate change projections for the Mediterranean
563 region. *Global and Planetary Change* 63: 90–104.
564 Gough, C.M., Vogel, C.S., Schmid, H.P., Su, H.B. and Curtis, P.S. 2008. Multi-year
565 convergence of biometric and meteorological estimates of forest carbon storage.
566 *Agricultural and Forest Meteorology* 148: 158–170.
567 Granda, E., Rossatto, D.R., Camarero, J.J., Voltas, J. and Valladares, F. 2014. Growth
568 and carbon isotopes of Mediterranean trees reveal contrasting responses to
569 increased carbon dioxide and drought. *Oecologia* 174: 307–317.
570 Grant, G.E., Tague, C.L. and Allen, C.D. 2013. Watering the forest for the trees: An
571 emerging priority for managing water in forest landscapes. *Frontiers in Ecology and*
572 *the Environment* 11: 314–321.
573 Guardiola-Claramonte, M., Troch, P.A., Breshears, D.D. et al. 2011. Streamflow
574 response in semi-arid basins following drought-induced tree die-off: Indirect climate
575 impact on hydrology. *Journal of Hydrology* 406: 225–233.

576 Hewitt, C.D. and Griggs, D.J. 2004. Ensembles-based predictions of climate changes
577 and their impacts. *Eos* 85: 566.
578 Hoerling, M. et al. 2012. On the increased frequency of mediterranean drought. *Journal*
579 *of Climate* 25: 2146–2161.
580 Jones, R.J.A., Hiederer, R., Rusco, E., Loveland, P.J. and Montanarella, L. 2004. *The*
581 *map of organic in topsoils in Europe, Version 1.2*. Septembre 2003: Explanation of
582 Special Publication Ispra 2004 No. 72 (S.P.I.04.72). European Soil Bureau Research
583 Report No. 17, EUR 21209 EN, 26pp. and 1 map in ISO B1 format. Office for
584 Official Publications of the European Communities. Luxembourg.
585 Jump, A.S., Hunt, J.M., Peñuelas, J., 2006. Rapid climate change-related growth decline
586 at the southern range edge of *Fagus sylvatica*. *Global Change Biology* 12: 2163–
587 2174.
588 Kong, G., Luo, T., Liu, X., Zhang, and Liang, L. 2012. Annual ring widths are good
589 predictors of changes in net primary productivity of alpine *Rhododendron* shrubs in
590 the Sergyemla Mountains, southeast Tibet. *Plant Ecology* 213: 1843–1855.
591 Lévesque, M., Saurer, M., Siegwolf, R., Eilmann, B., Brang, P., Bugmann, H. and
592 Rigling, A. 2013. Drought response of five conifer species under contrasting water
593 availability suggests high vulnerability of Norway spruce and European larch.
594 *Global Change Biology* 19: 3184–3199.
595 Lévesque, M., Siegwolf, R., Saurer, M., Eilmann, B. and Rigling, A. 2014. Increased
596 water-use efficiency does not lead to enhanced tree growth under xeric and mesic
597 conditions. *New Phytologist* 203: 94–109.
598 Linares, J.C. and Camarero, J.J. 2012a. Growth patterns and sensitivity to climate
599 predict silver fir decline in the Spanish Pyrenees. *European Journal of Forest*
600 *Research* 131: 1001–1012.

601 Linares, J.C. and Camarero, J.J. 2012b. From pattern to process: linking intrinsic water-
602 use efficiency to drought-induced forest decline. *Global Change Biology* 18: 1000–
603 1015.
604 Lloyd, A.H., Duffy, P.A. and Mann, D.H. 2013. Nonlinear responses of white spruce
605 growth to climate variability in interior Alaska. *Canadian Journal of Forest*
606 *Research* 43: 331–343.
607 López-Moreno, J.I., García-Ruiz, J.M. and Beniston, M. 2008. Environmental Change
608 and water management in the Pyrenees. Facts and future perspectives for
609 Mediterranean mountains. *Global and Planetary Change* 66: 300–312.
610 López-Moreno, J.I., Beniston, M. 2009. Daily precipitation intensity projected for the
611 21st century: Seasonal changes over the Pyrenees. Theoretical and Applied
612 Climatology 95: 375-384.
613 López Moreno, J.I., Goyette, S., Vicente-Serrano, S.M. and Beniston M. 2011. Effects
614 of climate change on the intensity and frequency of heavy snowfall events in the
615 Pyrenees. *Climatic Change* 105: 489–508.
616 Maherali H., Pockman W.T. and Jackson R.B. 2004. Adaptive variation in the
617 vulnerability of woody plants to xylem cavitation. Ecology, 85: 2184-2199.
618 Malmström, C.M., Thompson, M.V., Juday, G.P., Los, S.O., Randerson, J.T., Field,
619 C.B. 1997. Interannual variation in global-scale net primary production: Testing
620 model estimates. *Global Biogeochemical Cycles* 11: 367–392.
621 Martínez-Vilalta, J., López, B.C., Adell, N., Badiella, L. and Ninyerola, M. 2008.
622 Twentieth century increase of Scots pine radial growth in NE Spain shows strong
623 climate interactions. *Global Change Biology* 14: 2868–2881.

624 Martínez-Vilalta, J and Piñol, J. 2002. Drought-induced mortality and hydraulic
625 architecture in pine populations of the NE Iberian Peninsula. Forest Ecology and
626 Management 161: 247-256.
627 Medlyn, B.E., Duursma, R.A. and Zeppel, M.J.B. 2011. Forest productivity under
628 climate change: A checklist for evaluating model studies. *Climate Change* 2: 332–
629 355.
630 Mitchell, S., Csillag, F. and Tague, C. 2005. Impacts of spatial partitioning in
631 hydroecological models: predicting grassland productivity with RHESSys.
632 *Transactions in GIS* 9: 421–442.
633 Morales, P., Sykes, M.T., Prentice, I.C., Smith, P., Smith, B. et al. 2005. Comparing and
634 evaluating process-based ecosystem model predictions of carbon and water fluxes in
635 major European forest biomes. *Global Change Biology* 11: 2211–2233.
636 Moriasi, D.N., Arnold, J.G., Van Liew, M.W., Bingner, R.L., Harmel, R.D. and Veith,
637 T.L. 2007. Model evaluation guidelines for systematic quantification of accuracy in
638 watershed simulations. *American Society of Agricultural and Biological Engineers*
639 50: 885–900.
640 Nash, J. E. and Sutcliffe, J.V. 1970. River forecasting through conceptual models part I
641 – A discussion of principles. *Journal of Hydrology* 10: 282–290.
642 Panagos, P., Van Liedekerke, M., Jones, A., Montanarella, L., 2012. European Soil
643 Data Centre (ESDAC): response to European policy support and public data
644 requirements. *Land Use Policy* 29 (2), 329-338.
645 Pasho, E., J.J. Camarero, M. de Luis and Vicente-Serrano, S.M. 2011. Impacts of
646 drought at different time scales on forest growth across a wide climatic gradient in
647 north-eastern Spain. *Agricultural and Forest Meteorology* 151: 1800–1811.

Peng, J.-J., He, X.-Y., Chen, Z.-J., Cui, M.-X., Zhang, X.-L., Zhou, C.-H. 2012. Responses of *Pinus tabulaeformis* forest ecosystem in North China to climate change and elevated CO_2: A simulation based on BIOME-BGC model and tree-ring data. Chinese Journal of Applied Ecology 23: 1733–1742.

Peñuelas J., Canadell J., Ogaya, R. 2011. Increased water-use efficiency during the 20th century did not translate into enhanced tree growth. Global Ecology and Biogeography 20: 597-608.

Phillips, O.L., Phillips, O.L., van der Heijden, G., Lewis, S.L. et al. 2010. Drought-mortality relationships for tropical forests. *New Phytologist*. 187: 631–646.

Poulter, B., Pederson, N., Liu, H., Zhu, Z., D'Arrigo, R., Ciais, P., Davi, N. and Wang, T. 2013. Recent trends in Inner Asian forest dynamics to temperature and precipitation indicate high sensitivity to climate change. *Agricultural and Forest Meteorology* 178–179: 31–45.

Running, S., Ramakrishna, N. and Hungerford, R. 1987. Extrapolation of synoptic meteorological data in mountainous terrain and its use for simulating forest evapotranspiration and photosynthesis. *Canadian Journal of Forest Research* 17: 472–483.

Sabaté, S., Gracia, C.A. and Sánchez, A. 2002. Likely effects of climate change on growth of *Quercus ilex, Pinus halepensis, Pinus pinaster, Pinus sylvestris* and *Fagus sylvatica* forests in the Mediterranean region. *Forest Ecology and Management* 162: 23–37.

Sarris, D., Christodoulakis, D. and Körner, C. 2007. Recent decline in precipitation and tree growth in the eastern Mediterranean. Global Change Biology 13: 1187–1200.

Singh, J., Knapp, H.V. and Demissie, M. 2004. Hydrologic modeling of the Iroquois River watershed using HSPF and SWAT. ISWS CR 2004-08. Champaign, Ill.:

673 Illinois State Water Survey. Available in:
674 www.sws.uiuc.edu/pubdoc/CR/ISWSCR2004-08.pdf.
675 Solomon, S., et al., 2007. Climate Change 2007. The Physical Science Basis.
676 Cambridge University Press, Cambridge.
677 Stoy, P.C., Richardson, A.D., Baldocchi, D.D., Katul, G.G. et al. 2009. Biosphere–
678 atmosphere exchange of CO_2 in relation to climate: a cross-biome analysis across
679 multiple time scales. *Biogeosciences* 6: 2297–2312.
680 Stephenson, N.L. 1990. Climatic control of vegetation distribution: the role of the water
681 balance. *The American Naturalist* 135: 649–670.
682 Tague, C.L. and L.E. Band. 2004. RHESSys: Regional Hydro-Ecologic Simulation
683 System -an object-oriented approach to spatially distributed modeling of carbon,
684 water, and nutrient cycling. *Earth Interactions* 8: 1–42.
685 Tague, C. and Heyn, K. and Christensen, L. 2009a. Topographic controls on spatial
686 patterns of conifer transpiration and net primary production under climate warming
687 in mountain ecosystems. *Ecohydrology* 2: 541–544.
688 Tague, C., L. Seaby, and Hope, A. 2009b. Modeling the eco-hydrologic response of a
689 Mediterranean type ecosystem to the combined impacts of projected climate change
690 and altered fire frequencies. *Climatic Change* 93: 137–155.
691 Tague CL, McDowell NG, Allen CD. 2013. An integrated model of environmental
692 effects on growth, carbohydrate balance, and mortality of *Pinus ponderosa* forests in
693 the Southern Rocky Mountains. PLoS ONE 8: e80286.
694 doi:10.1371/journal.pone.0080286
695 Tague, C. and Peng, H. 2013. The sensitivity of forest water use to the timing of
696 precipitation and snowmelt recharge in the California Sierra: Implications for a

warming climate. *Journal of Geophysical Research G: Biogeosciences* 118: 875–887.

van Mantgem, P.J. and Stephenson, N.L. 2007. Apparent climatically induced increase of tree mortality rates in a temperate forest. *Ecology Letters* 10: 909–916.

Vicente-Serrano, S.M., Lasanta, T. and Gracia, C. 2010a. Aridification determines changes in leaf activity in *Pinus halepensis* forests under semiarid Mediterranean climate conditions. *Agricultural and Forest Meteorology* 150: 614–628.

Vicente-Serrano, S.M., Beguería, S., Juan I. López-Moreno, Miguel A. García-Vera and P. Stepanek. 2010b. A complete daily precipitation database for North-East Spain: reconstruction, quality control and homogeneity. International Journal of Climatology 30: 1146-1163.

Vicente-Serrano, S.M., Beguería, S. and López-Moreno, J.I. 2010c. A multiscalar drought index sensitive to global warming: The standardized precipitation evapotranspiration index. *Journal of Climate* 23: 1696–1718.

Vicente-Serrano, S.M., Beguería, S., Lorenzo-Lacruz, J., Camarero, J.J., López-Moreno, J.I., Azorín-Molina, C., Revuelto, J., Morán-Tejeda, E. and Sánchez-Lorenzo, A. 2012a. Performance of drought indices for ecological, agricultural and hydrological applications. *Earth Interactions* 16: 1–27.

Vicente-Serrano, S.M., Gouveia, C., Camarero, J.J., Beguería, S. et al. 2012b. Response of vegetation to drought time-scales across global land biomes. *Proceedings of the National Academy of Sciences of the United States of America* doi: 10.1073/pnas.1207068110.

Vicente-Serrano, S.M., Azorin-Molina, C., Sanchez-Lorenzo, A., Morán-Tejeda, E., Lorenzo-Lacruz, J., Revuelto, J., López-Moreno, J.I. and Espejo. F. 2014. Temporal

721 evolution of surface humidity in Spain: recent trends and possible physical
722 mechanisms. *Climate Dynamics* 42: 2655–2674
723 Williams, PA., Allen, C. D., Macalady, A. K., Griffin, D. et al. 2013. Temperature as a
724 potent driver of regional forest drought stress and tree mortality. *Nature Climate*
725 *Change* 3: 292–297.
726 Wösten, J.H.M., Lilly, A., Nemes, A. and Le Bas, C. 1999. Development and use of a
727 database of hydraulic properties of European soils. *Geoderma* 90: 169–185.
728 Zweifel, Z., Eugster, W., Etzold, S., Dobbertin, M., Buchmann, N. and Häsler, R. 2010.
729 Link between continuous stem radius changes and net ecosystem productivity of a
730 subalpine Norway spruce forest in the Swiss Alps. *New Phytologist* 187: 819–830.
731

	NSE	*r*	PBIAS (%)	RSR
Calibration period (1996-2006)	0.82	0.92	-12.6	0.06
Verification period (1986-1996)	0.61	0.82	-0.05	0.09

Table 1. Statistics of the calibration and verification periods show a good agreement between observed and predicted streamflow values obtained by the RHESSys hydro-ecological model as several statistics indicate (NSE; Nash-Sutcliff efficacy index; *r*, Pearson correlation coefficient; PBIAS, percent bias; RSR, ratio of the root mean square error to the standard deviation of measured data).

Figures

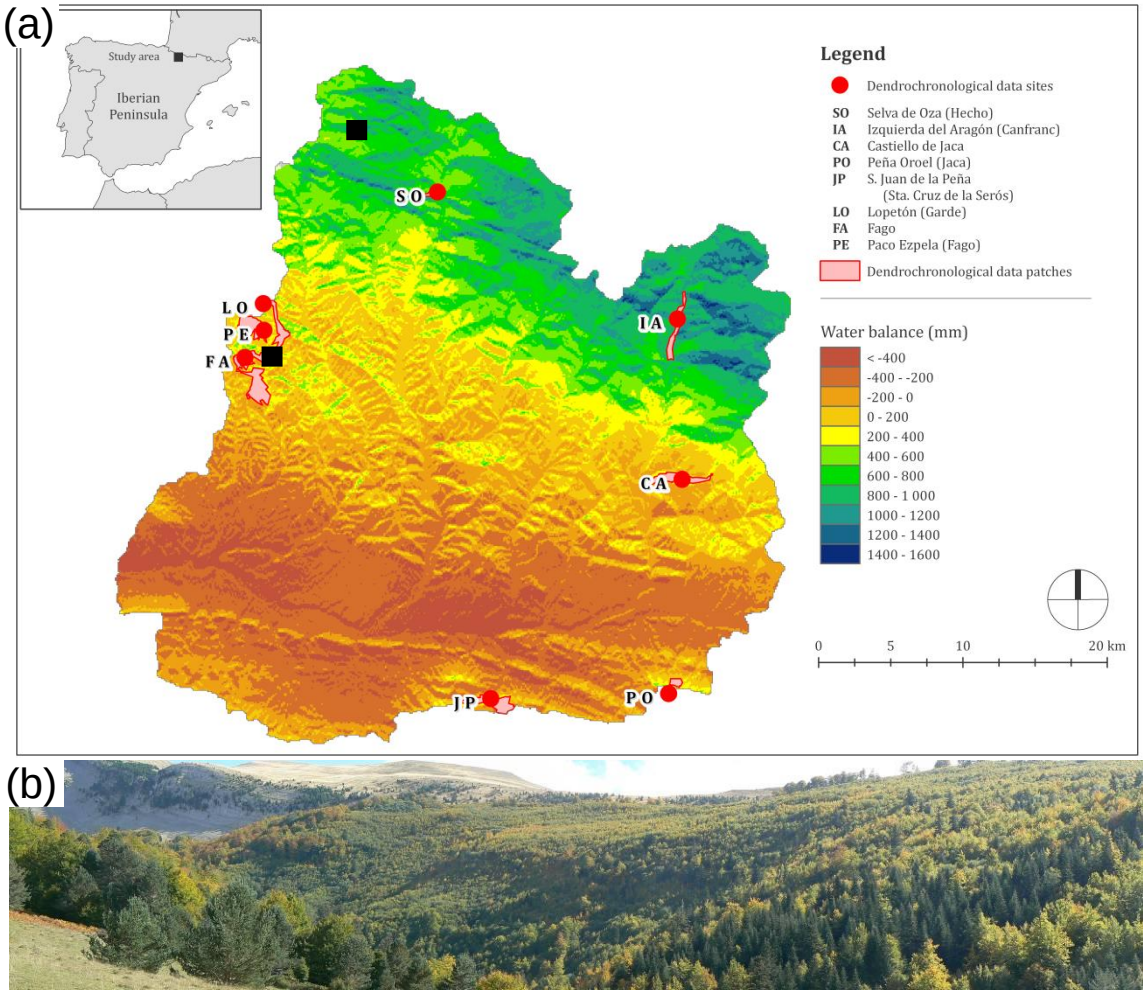

Figure 1. Study area located in the Spanish Pyrenees (Aragón) (a) and view of a mixed silver-fir-beech forest (Las Eras) located near the upper black square on the map. The red symbols correspond to the eight silver fir forests with available tree-ring width series, while red polygons indicate the forest patches simulated by the model RHESSys. The black symbols show the two study forests were intrinsic water-use efficiency was also estimated. Note the sharp gradient of annual water balance indicated by the brown-to-blue scale corresponding to a shift from dry to wet conditions as elevation increases northwards.

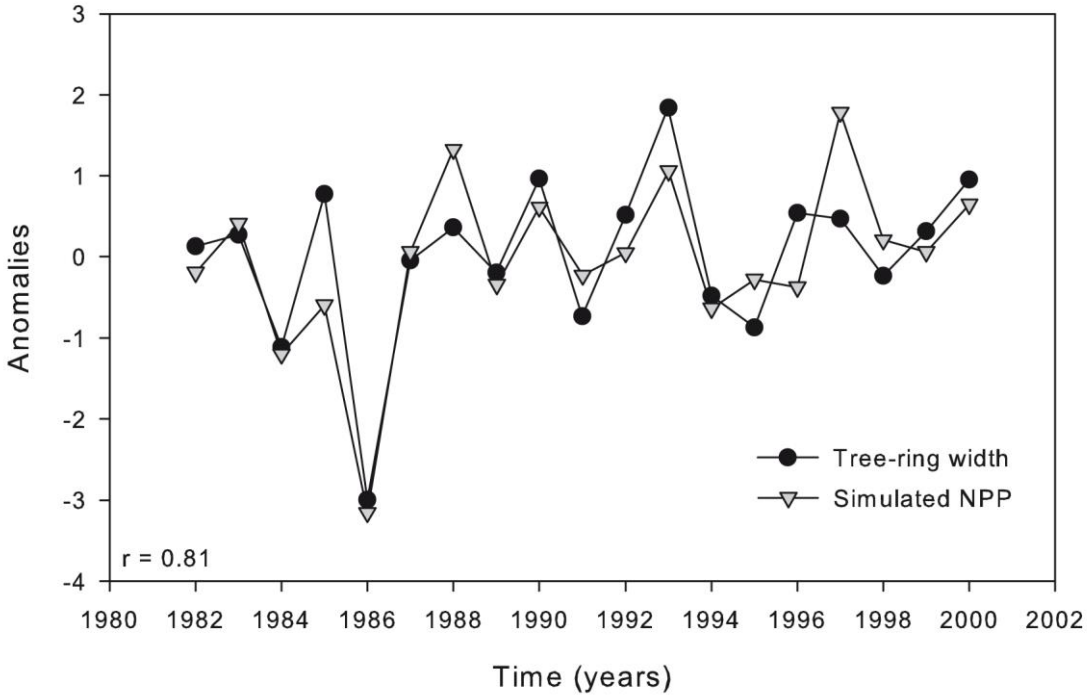

Figure 2. The regional tree-ring width index series of silver fir (continuous line) and the simulated net primary production (NPP) accumulated during 19 months until April (presented as anomalies, dotted line) are tightly and positively associated ($r = 0.81$, $P < 0.001$).

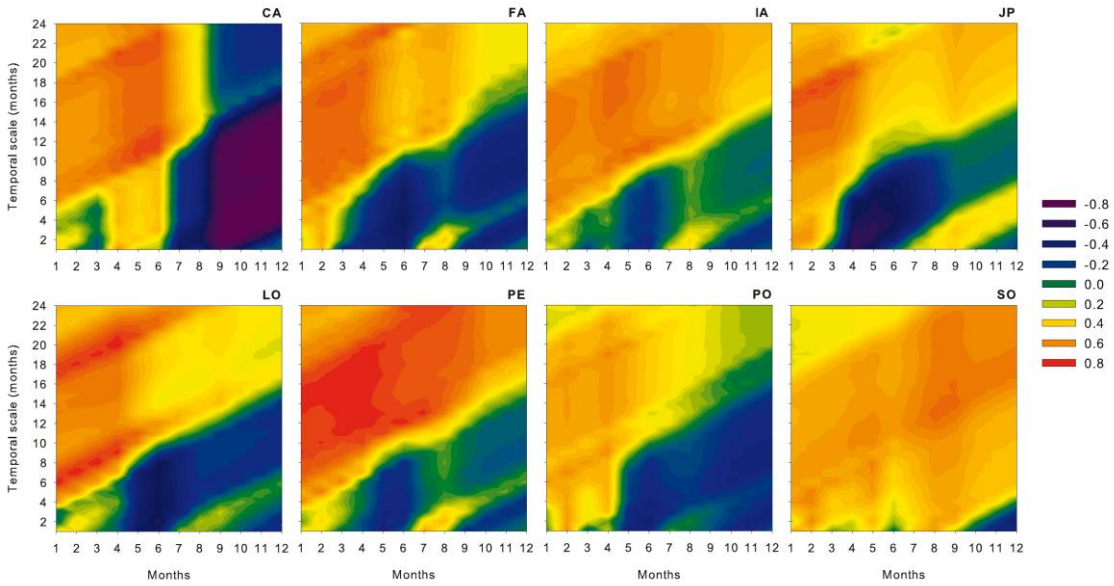

761

762 **Figure 3.** Local associations (Pearson correlation coefficients) observed between
763 simulated net primary production (NPP accumulated during 11 months until June of the
764 growth year) and the local tree-ring width series for the eight studied silver fir forests
765 (see sites' codes in Fig. 1). Correlations were calculated for temporal scales varying
766 from 1 to 24 months (*y* axes).

767

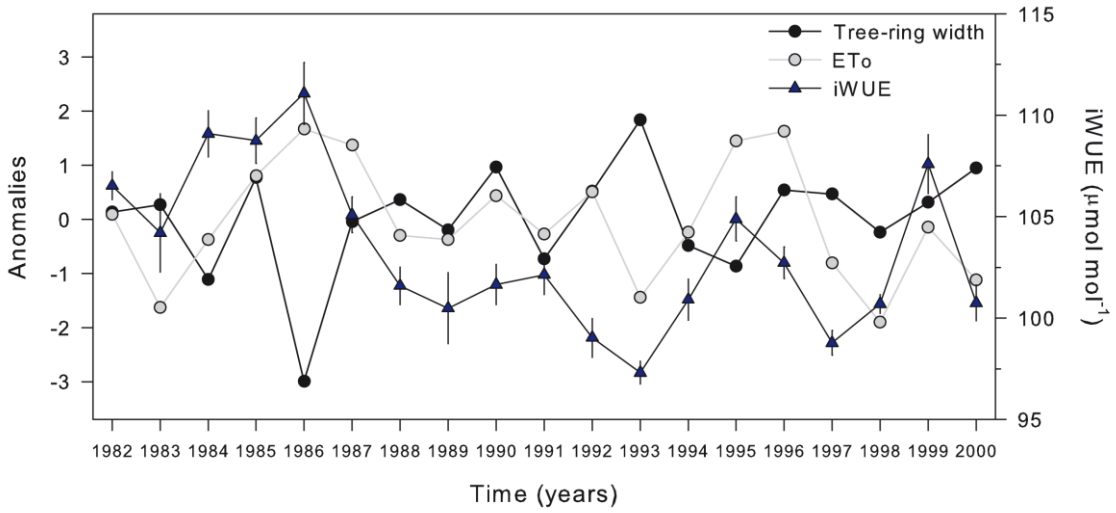

Figure 4. Comparison of the regional tree-ring width index and water-use efficiency (iWUE, mean ± SE) series and the evapotranspiration deficit or difference between reference (ETo) and actual evapotranspiration (ET). The tree-ring width indices and the evapotranspiration deficit are presented as anomalies. The correlation coefficients (significance levels) calculated between tree-ring width or iWUE and the water balance are r=-0.59 (P<0.05) and r=-0.79 (P<0.01), respectively.

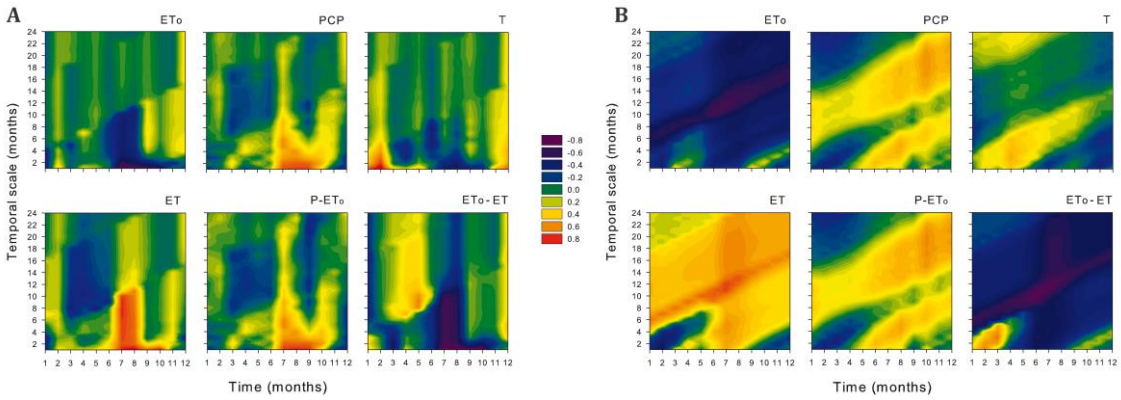

Figure 5. Correlations calculated at different temporal scales (1-24 months, *y* axes) between monthly climatic variables (ETo, reference evapotranspiration; PCP, precipitation; T, mean temperature; ET, evapotranspiration; P-ETo, water balance or difference between precipitation and reference evapotranspiration; ETo-ET, evapotranspiration deficit -difference between reference and actual evapotranspiration-) and simulated net primary production (NPP) (a) or growth data (b). x-axis in the plots correspond to the different months of the year (1 = Jan) and y-axis are the number of months preceding (x) for which climate variables were aggregated

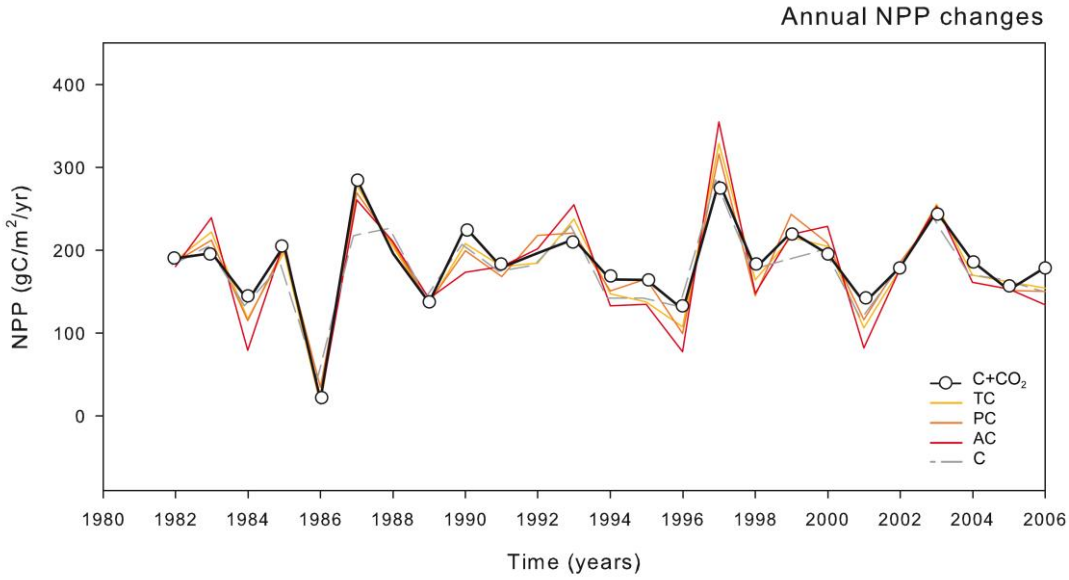

788

789 **Figure 6.** Evolution of the simulated regional NPP and the predicted NPP considering
790 three different climatic and emission scenarios to force observed regional climate
791 evolution between 1982 and 2006 ($C+CO_2$, control climate + 2050s projected
792 atmospheric CO_2 concentrations; TC, temperature change through a +3˚C warming; PC,
793 –20% precipitation change; and AC, combined +3˚C warming and –20% precipitation
794 decline, all these climate scenarios also consider the simulated atmospheric CO_2
795 concentrations for 2050; C, control climate and no change in atmospheric CO_2
796 concentrations).

797

Supplementary Material

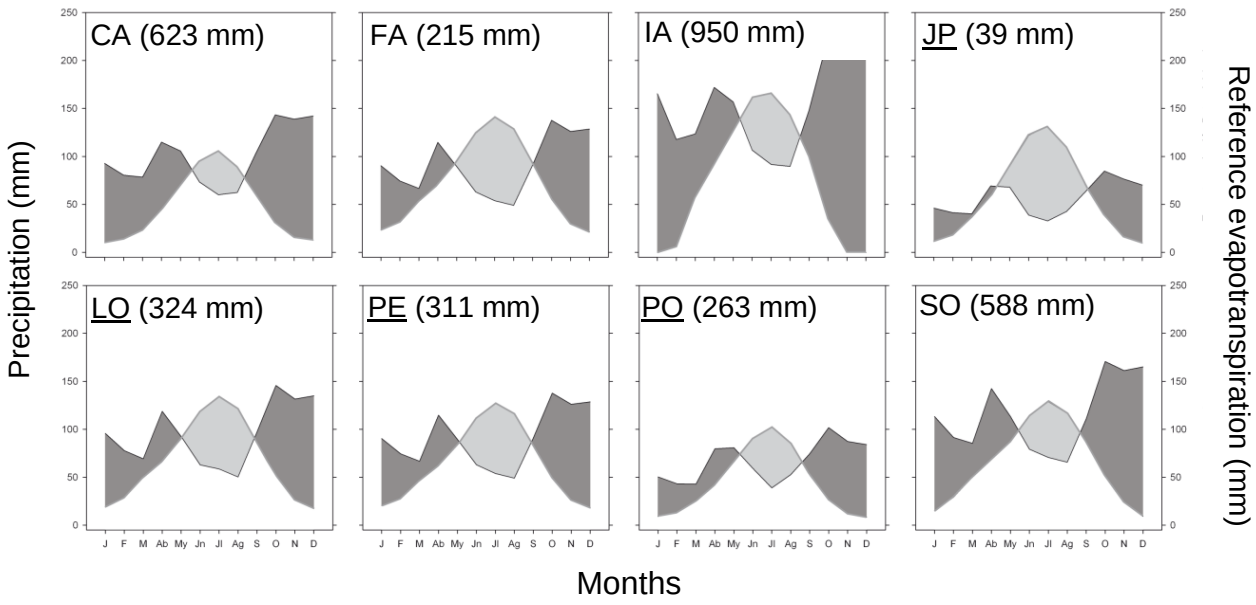

Figure S1. The study area encompasses a wide climatic gradient regarding the water balance. Diagrams showing monthly total precipitation (left y axis) and reference evapotranspiration (right y axis) monthly values for the eight studied forests. Dark and clear grey areas indicate positive and negative water balances (differences between P and ETo), respectively. The values shown in the upper left corner indicate the water balance estimated for each forest. Underlined codes correspond to sites showing die-off (see sites in Fig. S2).

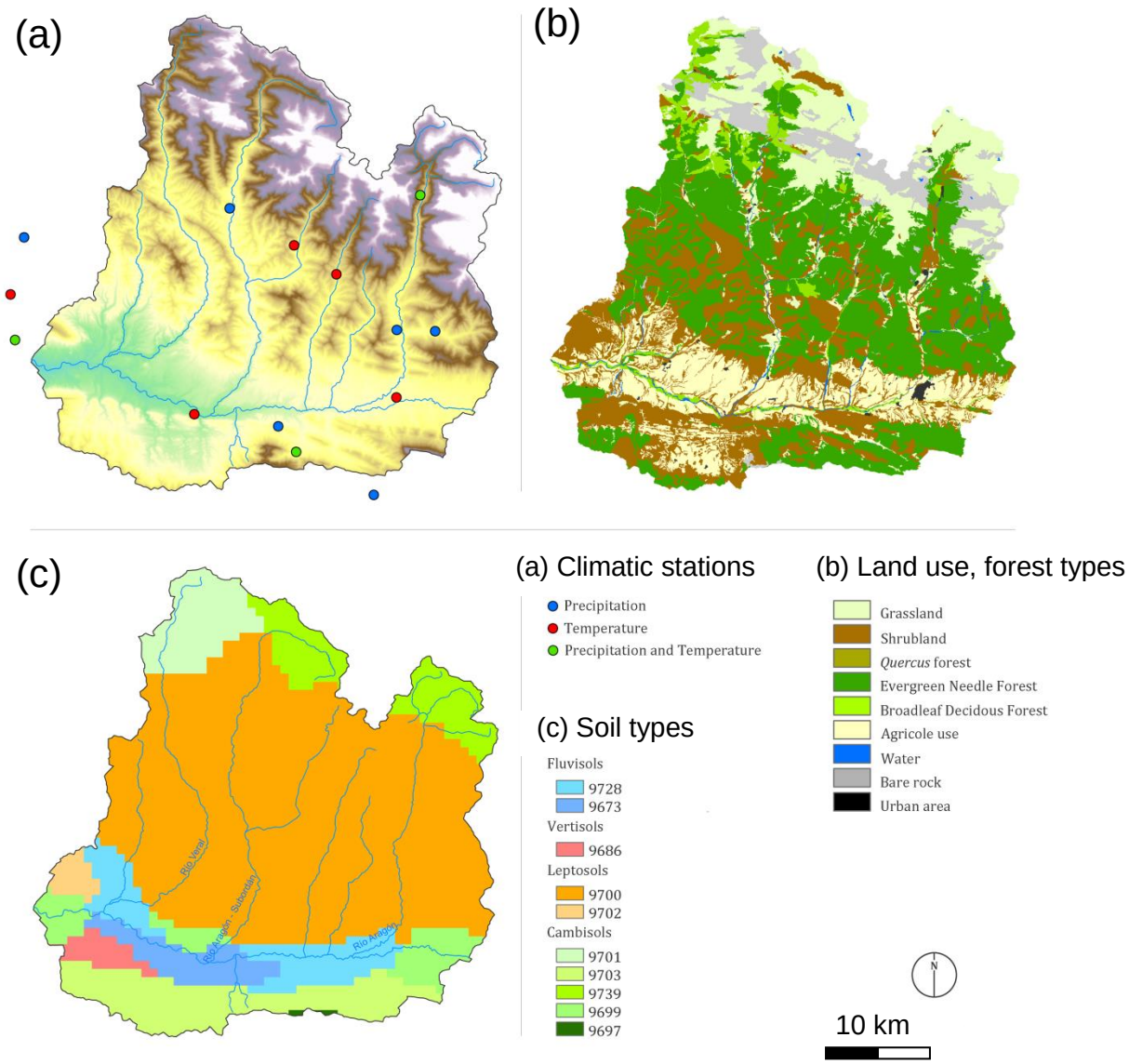

Figure S2. Geographical datasets used as inputs of the model RHESSys model including: (a) precipitation (blue dots) and temperature (red dots) data taken from meteorological stations, (b) forest types (data from the National Forest Map and the Third National Forest Inventory), and (c) soil classes.

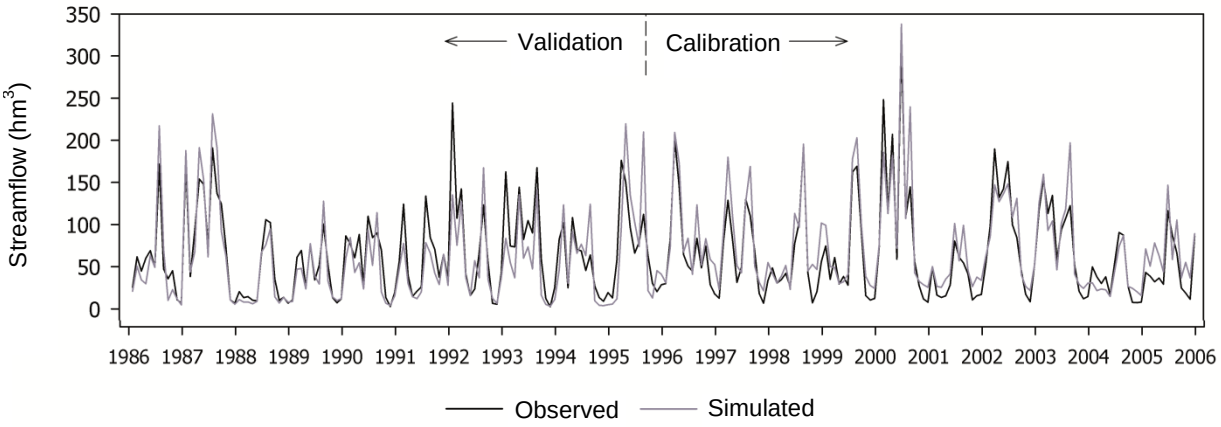

Figure S3. Observed (black line) and simulated (grey line) monthly streamflows in the study area (period 1986-2006). The figure shows the validation and calibration periods.

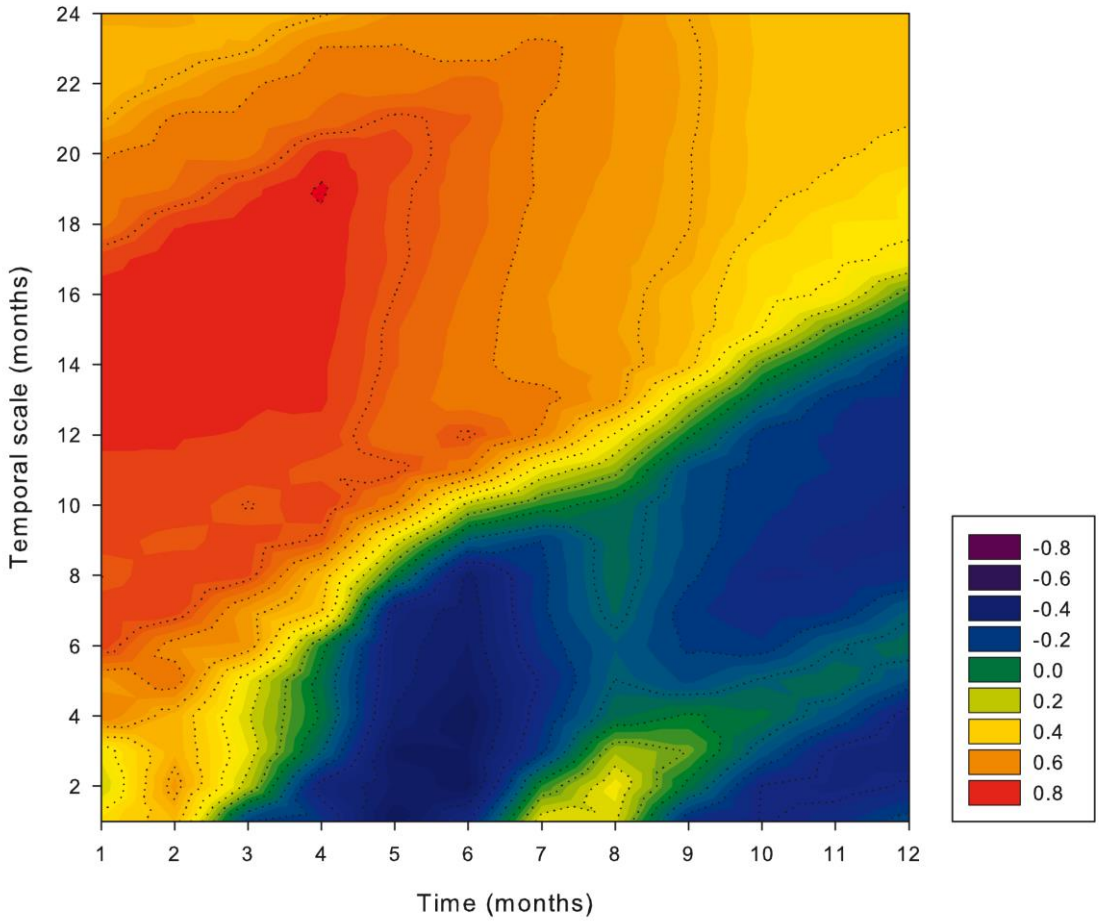

Figure S4. Pearson correlation coefficients (color scale) calculated at different temporal scales (*y* axis) between the regional tree-ring width index series and corresponding net primary production anomalies

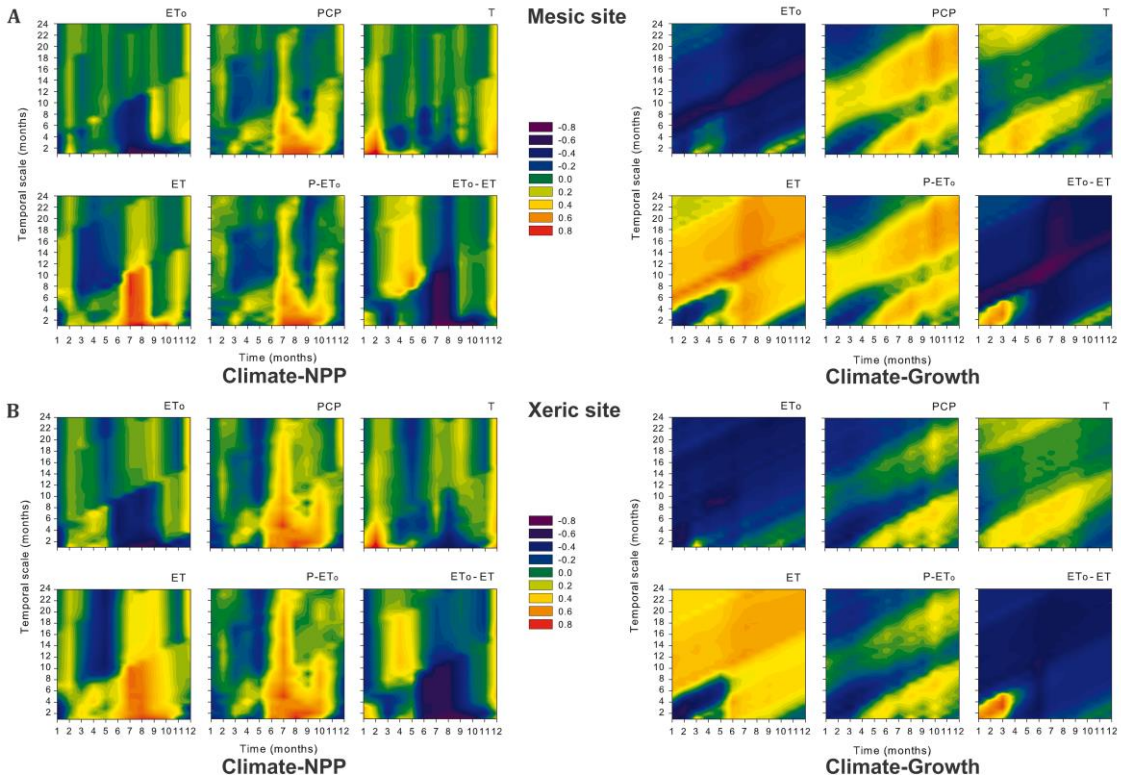

Figure S5. Correlations calculated at different spatial scales between monthly climatic variables (ETo, reference evapotranspiration; PCP, precipitation; T, mean temperature; ET, evapotranspiration; P-ETo, water balance or difference between precipitation and reference evapotranspiration; ETo-ET, evapotranspiration deficit −the difference between reference and actual evapotranspiration) and simulated net primary production or local tree-ring width indices (radial growth) for two forests with contrasting climatic conditions: mesic (a, site SO in Fig. 1) and xeric site (b, site JP in Fig. 1).

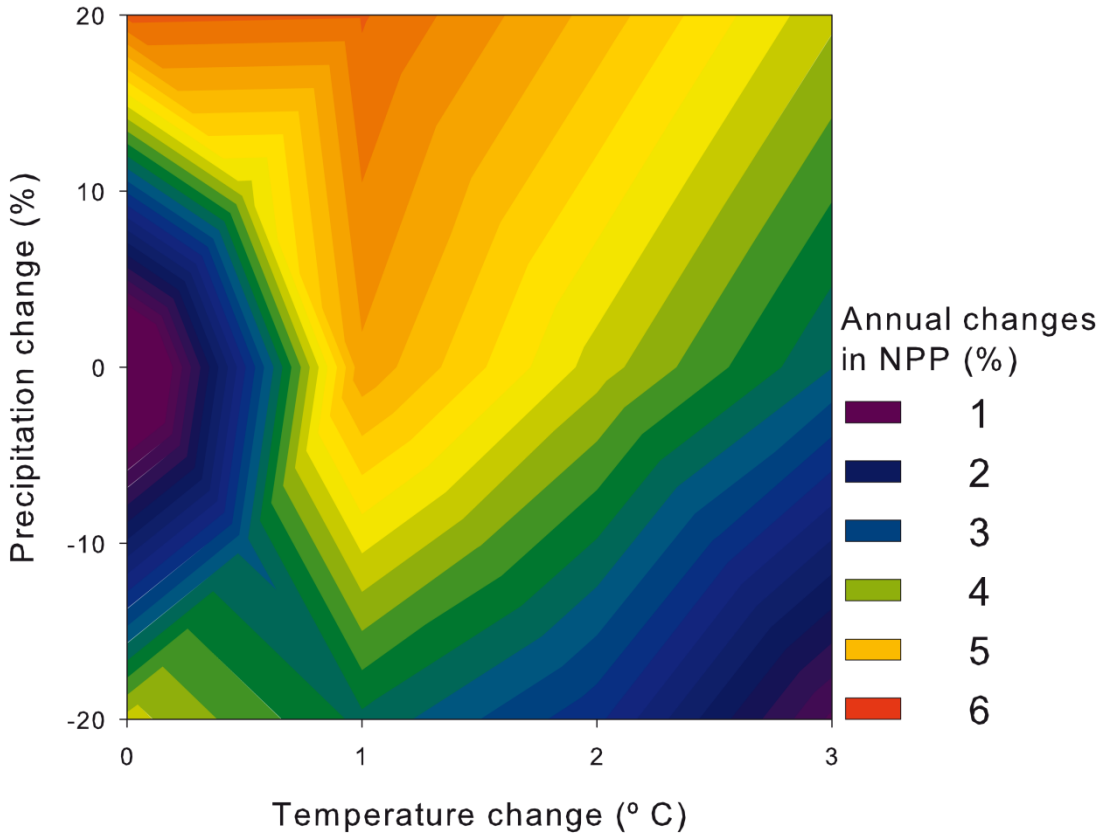

Figure S6. Relative responses (percentages) of the regional simulated net primary production (NPP) averaged over the simulation period to projected changes in mean air temperature and total precipitation (presented as percentage of the average values recorded in the study area).

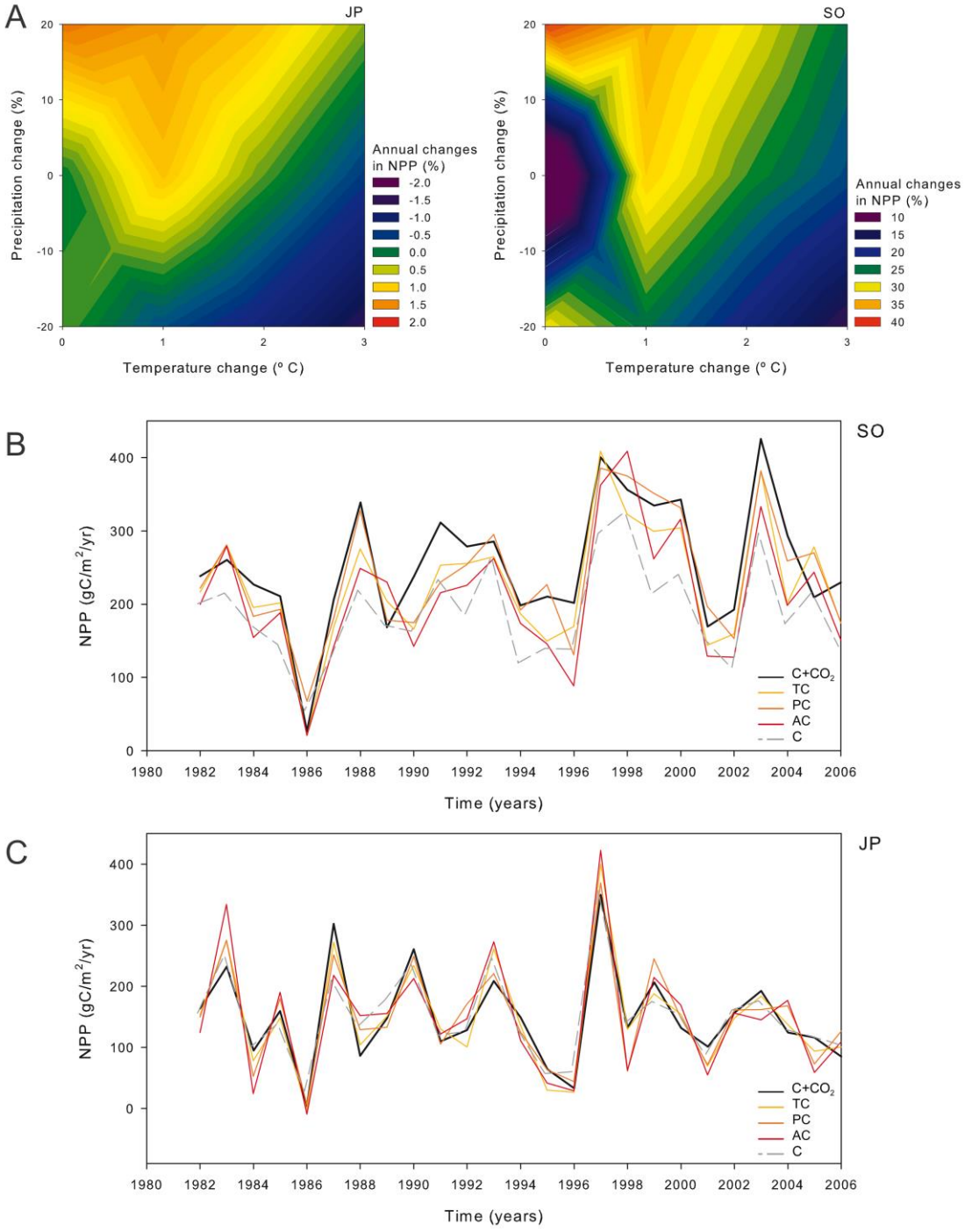

Figure S7. (A) Relative responses (percentages) of the regional simulated net primary production (NPP) anomalies to changes in mean temperature and total precipitation (presented as percentage of the maximum values recorded in the study area) in the xeric declining site JP showing die-off and the mesic non-declining site SO. The lower two figures show the evolution of the observed and predicted NPP values considering three different climatic scenarios ($C+CO_2$, control climate + 2050s projected atmospheric CO_2 concentrations; TC, temperature change through a +3 ˚C warming; PC, –20% precipitation change; and AC, combined +3˚C warming and –20% precipitation decline,

all these climate scenarios also consider the simulated atmospheric CO_2 concentrations for 2050; C, control climate and no change in atmospheric CO_2 concentrations) in sites SO (B) and JP (C).